NUMERICAL ANALYSIS OF FLOW FIELD INSIDE AND NEAR ERODED PART OF BANK

S. M. Habibullah BAHAR[1], Satoshi Yamagata[2] and Shoji FUKUOKA[3]

[1] Student Member of JSCE, Graduate Student, Department of Civil and Environmental Engineering, Hiroshima University (1-4-1 Kagamiyama, Higashi Hiroshima City, 739-8527, Japan)
[2] Member of JSCE, Hokkaido Development Bureau, (Hakodate City, 040-8501, Okawa – cho, 1-27, Japan)
[3] Fellow of JSCE, Dr. of Eng., Professor, Department of Civil and Environmental Engineering, Hiroshima University (1-4-1 Kagamiyama, Higashi Hiroshima City, 739-8527, Japan)

Flow near riverbank erosion was examined to investigate mechanism of bank erosion through experimental study of flow field of model bank erosion shape in the authors' previous study. This paper presents prediction of flow field near bank erosion. A numerical model is developed to compute two dimensional flow velocity and water depth for different model bank erosion shapes. The purpose of this study is to reproduce measured flow field of the model bank erosion shape. Curvilinear coordinate system is used in this analysis to obtain the bank erosion shape appropriately. The model could predict the flow field inside bank erosion for small erosion surface angle (equal or less then 4 degrees) with higher accuracy. It is also able to reproduce flow field inside erosion part for larger erosion surface angle (8 degrees), but absolute value of the computed velocity is larger than the measured velocity.

Key Words: *Erosion mechanism, riverbank of cohesive soil, erosion surface angle, bank erosion shape, 2-D horizontal flow field*

1. INTRODUCTION

Erosion process of cohesive riverbank has been studied through different approaches, such as, soil properties and their interactions, gravity forces and hydraulics of flow near bank surface. The hydraulic properties near bank have significant influence on cohesive riverbank erosion process. Because of long time accumulation of cohesive fine particle, riverbank may possesses vertical shape. Erosion process of this type of vertical bank was studied by laboratory investigation and field observation[1] through digging channel of natural river flood plain to investigate mechanism of bank erosion and to estimate erosion rate.

Fukuoka et al[2] studied the progress of cohesive bank erosion through laboratory experiment of undisturbed soil sample collected from flood channel of Yoshino River, Shikoku, Japan. It studied expansion mechanism of erosion area with change of hydraulic condition and continuos flow. As the bank material was composed of fine clay and sand, loose particles on bank surface were eroded first. Erosion area expanded in the upstream and downstream of the initially eroded locations. The progress of erosion continued until the erosion stagnated and the riverbank attained a stable condition. At some stage of erosion process, collapse of overhanging banks was observed. It was also observed that bank erosion depth and amount at near water surface was larger compared to those of under water surface bank erosion. It studied longitudinal change of velocity through a hydraulic model reproduced for an erosion shape of Yoshino River soil sample.

From erosion experiment of Yoshino River field sample (Fukuoka et al[3]), it was observed that maximum erosion depth and upstream erosion surface angle became gradually steeper. The upstream erosion surface angle was 5^0 to 9^0. At about 9^0, the angle and the erosion depth became stable. Based on the result of erosion experiment of field sample from Yoshino River, Fukuoka et al[2] reproduced model bank erosion shape to measure velocity in detail inside and near eroded part of overhanging bank. The velocity measurement during soil sample erosion experiment was not possible because of changing bank shape. The model bank erosion shape had same scale as the erosion experiment of Yoshino River soil sample. Hydraulic conditions of the model experiments were also similar to the experiments of collected soil samples. The flow fields near and inside bank erosion were measured through the model bank

Continuity Equation

$$\frac{\partial h}{\partial t}+\frac{\partial u^{\xi}h}{\partial \xi}+\frac{\partial u^{\eta}h}{\partial \eta}+\frac{u^{\xi}h}{r_{\xi}}+\frac{u^{\eta}h}{r_{\eta}}=0 \tag{1}$$

Momentum equation in the ξ direction

$$\frac{\partial u^{\xi}h}{\partial t}+\frac{\partial u^{\xi}u^{\xi}h}{\partial \xi}+\frac{\partial u^{\xi}u^{\eta}h}{\partial \eta}+\frac{\left(u^{\xi}u^{\xi}-u^{\eta}u^{\eta}\right)h}{r_{\xi}}+2\frac{u^{\xi}u^{\eta}h}{r_{\eta}}$$
$$=-gh\frac{\partial H}{\partial \xi}+\frac{\partial}{\partial \xi}\left(\nu_t h\frac{\partial u^{\xi}}{\partial \xi}\right)+\frac{\partial}{\partial \eta}\left(\nu_t h\frac{\partial u^{\xi}}{\partial \eta}\right)-\frac{\tau_{\xi b}}{\rho} \tag{2}$$

Momentum equation in the η direction

$$\frac{\partial u^{\eta}h}{\partial t}+\frac{\partial u^{\xi}u^{\eta}h}{\partial \xi}+\frac{\partial u^{\eta}u^{\eta}h}{\partial \eta}+\frac{\left(-u^{\xi}u^{\xi}+u^{\eta}u^{\eta}\right)h}{r_{\eta}}+2\frac{u^{\xi}u^{\eta}h}{r_{\xi}}$$
$$=-gh\frac{\partial H}{\partial \eta}+\frac{\partial}{\partial \xi}\left(\nu_t h\frac{\partial u^{\eta}}{\partial \xi}\right)+\frac{\partial}{\partial \eta}\left(\nu_t h\frac{\partial u^{\eta}}{\partial \eta}\right)-\frac{\tau_{\eta b}}{\rho} \tag{3}$$

erosion shape in laboratory and, investigated relationship between flow characteristics and erosion mechanism (Fukuoka et al[3]).

There have been many studies on cohesive bank erosion mechanism. But those are not enough to understand natural riverbank erosion mechanism. It is required to know flow field near and inside bank erosion accurately to estimate erosive resistance of cohesive soil against flow hydraulics, and to understand erosion mechanism. Because of scale effect, experimental study is not enough to understand bank erosion process and mechanism. It is very important to do numerical simulation in an objective to realize riverbank erosion mechanism. Until now, there are seldom numerical studies on the flow hydraulics inside riverbank erosion. Fukuoka et al[4] applied k-ε model for solving flow around overhanging bank. The model predicted vertical flow and well agreed with experimental flow in a curved channel with overhanging bank. In the studies about the numerical computation on the flow separation, Nezu et al[5] described turbulent and flow separation in cavity open-channel flow using large eddy simulation (LES). A 3-D and non-linear k-ε model was developed to calculate turbulent flow around a surface-mounted cubic obstacle. The Kimura et al's model reproduced separated and reattached flow around a cube. Again, Zhou et al[7] attempted to simulate separation and reattachment of unsteady flow around spur-dike using large eddy simulation (LES).

In this paper, the authors have attempted to reproduce horizontal velocity field and water depth of the model bank erosion shape done by Fukuoka et al[3]. A 2-Dimensional numerical model is developed to simulate velocity fields and flow separation inside the riverbank erosion, velocity distribution across the channel and water depth along the bank erosion. The model predicts the velocity field and water depth well for small erosion surface angle of 4 degrees. But for higher erosion surface angle of 8 degrees, absolute magnitude of velocity inside the bank erosion is over estimated.

2. GOVERNING EQUATIONS

The flow field inside the riverbank, which is hollow at left bank, is dominant in horizontal plane compared with the vertical direction. For this study, two-dimensional flow regime is approximated to understand cohesive riverbank erosion mechanism. Therefore, in this paper, a two-dimensional numerical model is developed to simulate with measured flow field of bank erosion model. Orthogonal curvilinear coordinate system is used in this analysis. Its downstream direction is ξ axis and right-angled cross-sectional direction is η axis. The governing equations of this numerical model are obtained by depth integration of continuity equation and Navier-Stokes equations (Eq.(1), (2) and (3)) in curvilinear coordinate.

Here, h = water depth, H = water level, u^{ξ}: velocity in ξ direction, u^{η}: velocity in η direction, n: Manning's roughness coefficient, ν_t: eddy viscosity coefficient, r_{ξ}: radius of curvature in axis, r_{η}: radius of curvature in axis

In the computation, 1st order convective terms are obtained by upstream finite difference of control volume. The shear stress due to difference in velocity for inside the erosion part and main flow part is expressed by diffusion term of momentum equation. It supposes that vortex viscosity

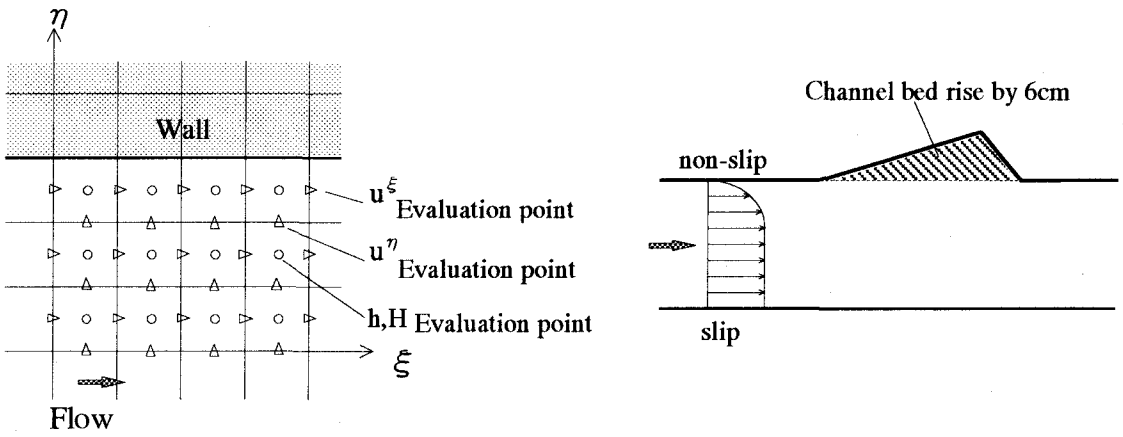

Fig. 1 Computational grid and evaluation point

coefficient ν_t is proportional to local frictional velocity u_* and water depth h. The viscosity coefficient ν_t is shown by following formula.

$$\nu_t = \frac{\kappa}{6} u_* h \tag{4}$$

Here, κ is Karman constant (=0.4). Bed shear stresses $\tau_{\xi b}$, $\tau_{\eta b}$ are shown by following equations using Manning's roughness coefficient n.

$$\tau_{\xi b} = \rho g \frac{n^2 u^{\xi} \sqrt{u^{\xi 2} + u^{\eta 2}}}{h^{1/3}} \tag{5}$$

$$\tau_{\eta b} = \rho g \frac{n^2 u^{\eta} \sqrt{u^{\xi 2} + u^{\eta 2}}}{h^{1/3}} \tag{6}$$

The frictional velocity u_* using bed shear stress is shown by following equation.

$$u_* = \sqrt{\frac{\tau_b}{\rho}} = \sqrt{g \frac{n^2 \left(u^{\xi 2} + u^{\eta 2}\right)}{h^{1/3}}} \tag{7}$$

All computational velocities are zero as initial condition. Discharge at upstream end, water depth at upstream and downstream end, channel slope and roughness was supplied as an input data in the program. Time steps of the computation were obtained by trial and error method for the meshes of different bank erosion shape. The computation became stable approximately after 100s elapse time, and its output was considered as computation result.

3. GRID AND BOUNDARY CONDITION

For this numerical analysis, staggered grid as shown in Fig. 1 is used for the computation. Because of the orthogonal curvilinear coordinate, the ξ axis passes along the erosion surface and crosses the η axis at right angle for each grid point. Locations of velocity components in ξ axis direction and η axis direction are also shown by arrows in the Fig. 1. Water depth is evaluated at center of control volume, and velocity components at ξ axis direction and η axis direction were calculated for the points on the faces of control volume. For computational mesh, enough number of grid points is necessary to reproduce an eddy inside the erosion part.

Table 1 Computational boundary condition

	Upstream erosion surface angle (degrees)	Flow rate (l/s)	Water depth at downstream (cm)
Case 1	8	36.7	14.5
Case 2	8	27.6	11.5
Case 3	8	21.5	9.6
Case 4	4	36.7	14.5

As the right bank of the channel was made of smooth glass, slip condition is applied during computation. On the other hand, the left bank side with bank erosion model was provided artificial roughness. Therefore, the computation for the left bank has non-slip condition. The Manning's roughness coefficient n for the channel bed and right bank is 0.0103 and 0.01 respectively. The n value for artificial roughness of the left bank is 0.025. Boundary conditions of this numerical simulation are shown in Table 1.

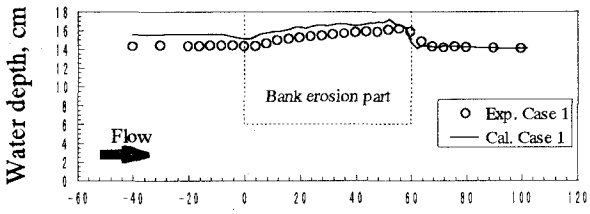

(a) Longitudinal water depth distribution.

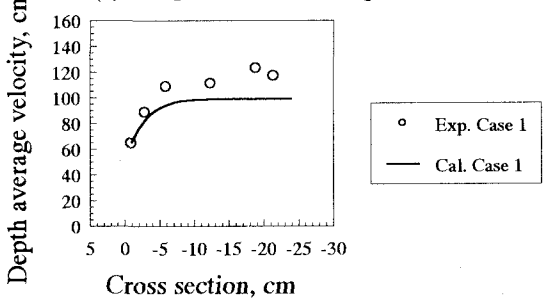

(b) Depth averaged velocity distribution across the channel at 40cm upstream of erosion part.

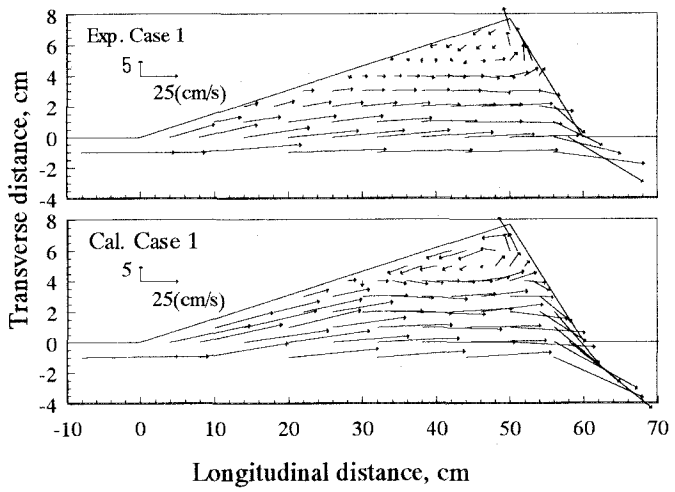

(c) Measured and computed depth averaged velocity vector.

Fig. 2 Computed and measured flow field of Case 1, 8^0 erosion surface angle.

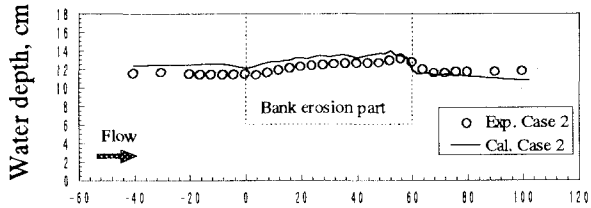

(a) Longitudinal water depth distribution.

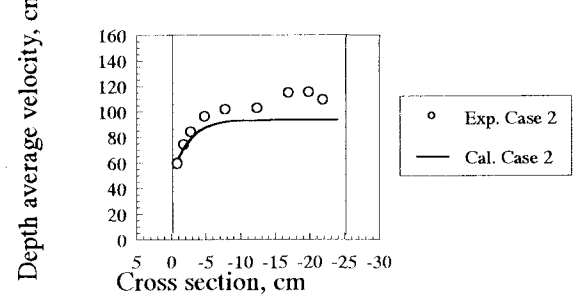

(b) Depth averaged velocity distribution across the channel at 40cm upstream of erosion part.

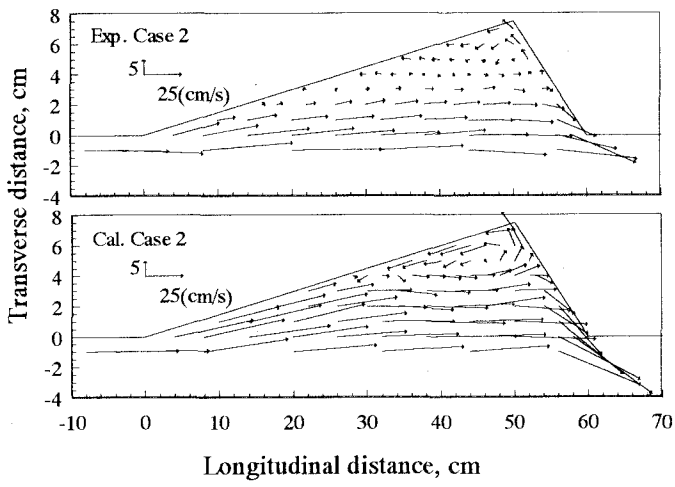

(c) Measured and computed depth averaged velocity vector.

Fig. 3 Computed and measured flow field of Case 2, 8^0 erosion surface angle.

4. MODEL BANK EROSION SHAPE

Erosion progress and its mechanism of undisturbed cohesive soil sample from Yoshino River flood channel Japan, was investigated (Fukuoka at al. [2]) through laboratory experiment. It was observed that erosion initiated first at locations of smaller resistive bank soil. The erosion continued in length and depth until attaining a stable shape. There were two types of bank erosion shapes: (a) near water surface bank erosion and (b) under water surface erosion. Among those two types of bank erosion shape, near water surface one was larger and most dominant for cohesive bank erosion. After initiation of flow, bank erosion length, depth and surface angle increased until attaining stable condition. The erosion surface angle varied from 4^0 to 8^0. Flow characteristics near bank erosion were studied[2), 3)] through model bank erosion shape having same scale as Yoshino river soil sample erosion experiment to understand relationship between flow field and erosion rate of cohesive soil.

In this study, numerical simulation is done for the measured flow field of near bank erosion type that exists near water surface. The bank erosion shape

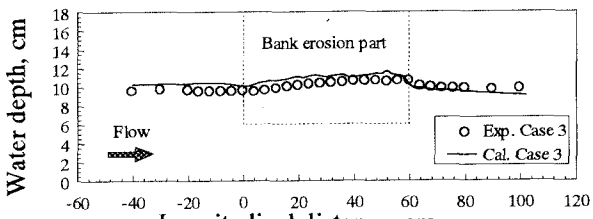

(a) Longitudinal water depth distribution

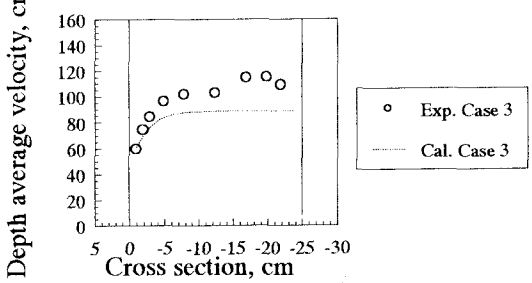

(b) Depth averaged velocity distribution across the channel at 40cm upstream of erosion part.

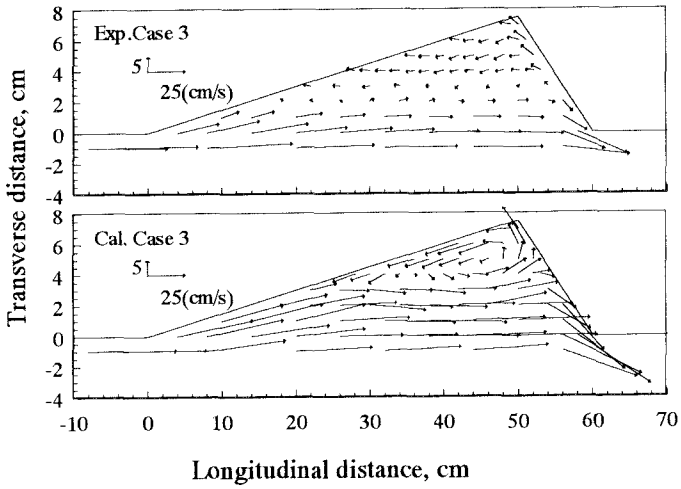

(c) Measured and computed depth averaged velocity vector.

Fig. 4 Computed and measured flow field of Case 3, 8^0 erosion surface angle.

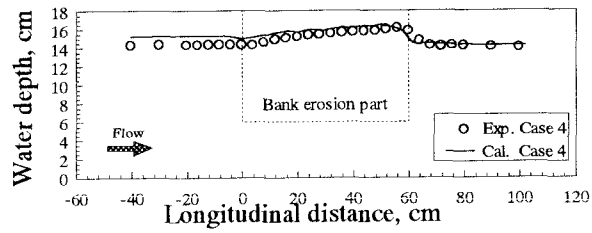

(a) Longitudinal water depth distribution.

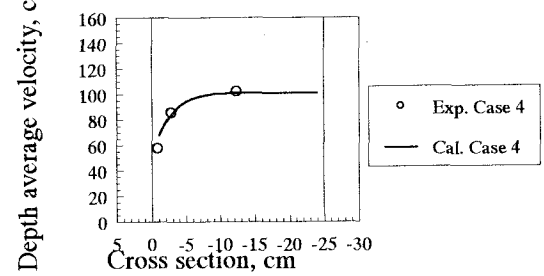

(b) Depth averaged velocity distribution across the channel at 40cm upstream of erosion part.

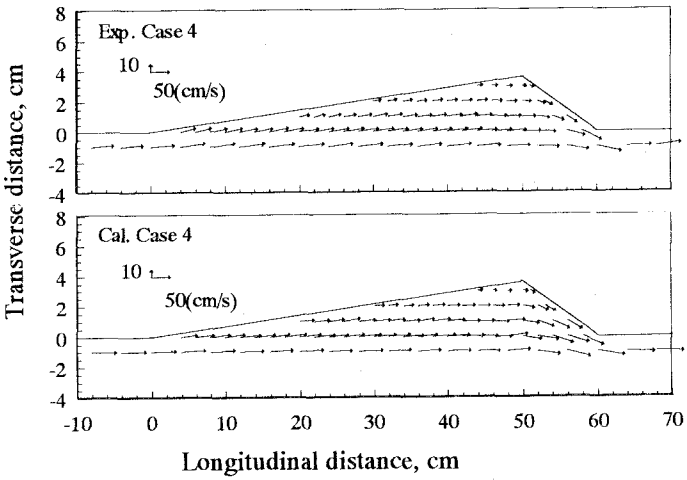

(c) Measured and computed depth averaged velocity vector.

Fig. 5 Computed and measured flow field of Case 4, 4^0 erosion surface angle.

varied in erosion surface angles 4 degrees and 8 degrees, and erosion length 60cm.

5. RESULT AND DISCUSSION

a) 8 degrees erosion surface angle

The Fig. 2 shows computational and experimental results of Case 1, which have 8 degrees erosion surface angle, 60cm erosion length and largest water discharge in the channel. Figure 2(a) compares water depth distribution along 1cm from left bank. The computational water depth shows a similar tendency as that of the measured, as it rises along bank erosion part and fall down from downstream erosion part towards lower reach of the channel. However, computed water depth at upstream and near the erosion part is equal or larger by 1 cm then the measured depth. At the same time, the water depth at upstream of the erosion part is little over predicted. It is suppose that, because of large erosion profile in the channel, its influence propagated to upper stream. Figure 2(b) is comparing distribution of depth average velocity across main channel section at 40cm upstream of the erosion part. Computational velocity near left bank side shows closeness to the experimental result.

On the contrary, Fig. 2(b) shows that there is difference of the measured and computed velocity by 20cm/sec near right bank side. It is because of larger computed water depth at upstream of the

erosion part as shown by the Fig. 2(a). Depth averaged velocity vector inside erosion part for measured and computed are shown in Fig. 2(c). Due to adverse pressure gradient starting from upstream of erosion part, both the computed and the measured velocity vector indicate flow separation near wall inside the bank erosion. The computational velocity vector differs in size from the measured velocity vector at that location of maximum erosion depth. As a result, the velocity inside the erosion part is larger and flow rate entering into the erosion part is over estimated than that of experiment. Higher velocity in the mainstream and complicated mixing of flow inside erosion part is the cause of over estimation. Further improvement of the model is required to predict the flow field inside and near bank erosion with more accuracy.

Figure 3 and 4 show computed and measured flow fields of Case 2 and Case 3. Their erosion surface angle and length is same as Case 1 (8 degrees and 60cm), but flow rate from upstream end is smaller than that of Case 1. The computational results of Case 2 and Case 3 show similar tendency as Case 1, computed water depths are larger and computed mainstream velocities are smaller than those of the measured. The velocity, which enters into erosion part is also over estimated. In Case 2 and Case 3, difference between the computed and the measured velocity vector in respect of size and eddy flow area is larger. In the computation, the water depth changes with flow rate, but the velocity vectors hardly change.

The flow separation, which occurs near the erosion surface, has a strong influence on velocity in the erosion part. It is influenced mainly by momentum exchanged between mainstream and erosion part. The experimental results show that there is larger flow separation area for lower water depth compared to that of higher water depth. Because, smaller volume of water in erosion part for lower depth is driven by momentum exchange between the main stream and the erosion part. The above analysis shows that there are significant differences between the computed and measured results. The reasons are that in the experimental case of the large erosion surface angle the flow field might be of 3-dimensional and there exits complicating flow mixing inside the erosion part. A 3-dimensional model might be desirable for the analysis of the flow field inside the bank erosion.

b) 4 degrees erosion surface angle

Simulation of Case 4 is shown in Fig. 5. This case has same boundary condition as Case 1, but different erosion surface angle of 4 degrees. Case 4 has 60cm erosion length. Water depth distribution of Fig. 5(a) reveals that difference between computed and measured water depth is very low for Case 4 of 4 degrees erosion surface angle. Again, velocity distribution across the channel (Fig. 5(b)) indicates that computed velocity well agrees with measured velocity in the upstream of the erosion part. At the same time, velocity vector of Fig. 5(c) shows that the computed and measured velocity vectors are similar. This is because of absent of flow separation inside the erosion part. Therefore, the model accurately predicts velocity field inside the erosion part for small erosion surface angle. Its accuracy becomes less for large erosion surface angle. Further development of the model is going on, so that it could predict flow field inside bank erosion to understand riverbank erosion mechanism.

6. CONCLUSIONS

This numerical study has attempted to simulate two dimensional horizontal flow field, longitudinal water depth distribution along bank erosion of near water surface and velocity distribution across the channel in upstream of bank erosion. The model could predict them accurately for small erosion surface angle. It also could reproduce the flow fields for higher erosion surface angle, but their absolute magnitudes were over estimated. Therefore, it requires further study to predict accurate scale of eddy flow inside the erosion part to understand cohesive riverbank erosion mechanism.

REFERENCES

1) Fukuoka, S.,: Erosion process of natural river bank, Proc. of 1st International Symposium on Hydraulic Measurement, Beijing, China, pp. 223-229, 1994-11.
2) Fukuoka, S., Watanabe, A., Katayama, T., Itaya, E., Kashiwagi, Y., Yamagata, S., and Hayashi, M.,: Erosion expansion mechanism of cohesive (silt) bank by the stream flow, Ann. J. Hydr. Engrg, JSCE, vol. 43, pp. 695-700, 1999. (in Japanese)
3) Fukuoka, S., Watanabe, A., Yamagata, S., and Kashiwagi, Y.,: Relation of flow velocity around riverbank and formation of overhanging bank, Ann. J. Hydr. Engrg, JSCE, vol. 44, pp. 759-764, 2000. (in Japanese)
4) Fukuoka, S., Daito, M., Nishimura, T., and Sato, K.,: Flow and bed profiles of channel with overhanging bank, JSCE, (533/II – 34), pp. 147-156, 1996-2. (in Japanese)
5) Nezu, I., and Yamamoto, Y.,: Study on the turbulent structures in cavity open-channel flows, J. Hydro. Coast. and Env. Engg., JSCE, (614 – II-46), pp. 51-63, 1999-2. (in Japanese)
6) Kimura, I., and Hosoda, T.,: Numerical analysis of flows around a cube by means of a non-linear k-ε model, Ann. J. Hydr. Engrg, JSCE, vol. 44, pp. 599-604, 2000. (in Japanese)
7) Zhou, Y., Michiue, M., and Hinokidani, O.,: A numerical method of 3-D flow around submerged spur-dikes, Ann. J. Hydr. Engrg, JSCE, vol. 44, pp. 605-610, 2000.

(Received October 2, 2000)